This article has been accepted for publication in Protein Engineering design and Selection Published by Oxford University Press. Doi: http://dx.doi.org/10.1093/protein/gzw066

# Production and Characterization of Functional Recombinant Hybrid Heteropolymers of Camel Hepcidin and Human Ferritin H and L Chains

**Mohamed Boumaiza[1*], Fernando Carmona[2], Maura Poli[2], Michela Asperti[2], Alessandra Gianoncelli[3], Michela Bertuzzi[3], Paola Ruzzenenti[2], Paolo Arosio[2] and Mohamed Nejib Marzouki[1]**

[1]Laboratoire d'ingénierie des protéines et des molécules bioactives, Institut Nationale des Sciences Appliquées et de Technologie (I.N.S.A.T.) BP 676, Tunis Cedex1080, Tunisie, [2]Molecular Biology Laboratory, Department of Molecular and Translational Medicine, University of Brescia, Viale Europa 11, Brescia, Italy, and [3]Proteomics Platform, Department of Molecular and Translational Medicine, University of Brescia, Viale Europa 11, Brescia, Italy

* To whom correspondence should be addressed. E-mail: m.boumaiza@yahoo.fr

**Keywords:** Camel hepcidin/human ferritin H and L chains/heteropolymers/J774 cells.

**Abbreviations:**

HepcH; fusion camel hepcidin-human ferritin H-chain subunit; FTH: human ferritin H; HepcH-FTH, 24-mer heteropolymer comprising camel hepcidin-human ferritin H assembled with FTH; FTL: human ferritin L; HepcH-FTL, 24-mer heteropolymer comprising camel hepcidin-human ferritin H assembled with FTL.

**Abstract**

Hepcidin is a liver-synthesized hormone that plays a central role in the regulation of systemic iron homeostasis. To produce a new tool for its functional properties the cDNA coding for camel hepcidin-25 was cloned at the 5'end of human FTH sequence into the pASK-IBA43plus vector for expression in *E. coli*. The recombinant fusion hepcidin-ferritin-H subunit was isolated as an insoluble iron-containing protein. When alone it did not refold in a 24-mer ferritin molecule, but it did when renatured together with H- or L-ferritin chains. We obtained stable ferritin shells exposing about 4 hepcidin peptides per 24-mer shell. The molecules were then reduced and re-oxidized in a controlled manner to allow the formation of the proper hepcidin disulfide bridges. The functionality of the exposed hepcidin was confirmed by its ability to specifically bind the mouse macrophage cell line J774 that express ferroportin and to promote ferroportin degradation. This chimeric protein may be useful for studying the hepcidin-ferroportin interaction in cells and also as drug-delivery agent.

## Introduction

There has been significant progress in identifying the molecules controlling iron homeostasis and their mode of action (Recalcati *et al*., 2010; Pantopoulos *et al*., 2012). Hepcidin is the key iron regulatory hormone (Ganz, 2003). It is a 25 amino acid peptide belonging to the β-defensin family, isolated for the first time from plasma and human urine (Krause *et al*., 2000; Park *et al*., 2001), and consists of a cysteine-rich cationic peptide engaged with four disulfide bridges which plays a major role in innate immunity and iron homeostasis (Falzacappa and Muckenthaler, 2005; Houamel *et al*., 2016). It is induced by iron abundance and inflammation and is suppressed by iron deficiency and hypoxia. Recently it has been reported that circulating hepcidin-25 is reduced by endogenous estrogen in humans (Lehtihet *et al*., 2016). Hepcidin binds and inhibits ferroportin1, the only cellular iron exporter (Ramey *et al*., 2010) and thus, high hepcidin reduces while low hepcidin increases systemic iron availability (Nemeth and Ganz, 2006). Furthermore, modulation of this peptide can offer promising clinical applications to treat iron deregulation (Blanchette *et al*., 2016). Hepcidin acts via its N-terminal domain of 7–9 amino acids, including a thiol cysteine, that is the minimal structure retaining hepcidin activity (Preza *et al*., 2011). The 3D structure of human hepcidin is known (Jordan *et al*., 2009). Recombinant human and mouse hepcidins were expressed in *E. coli* in fusion with a thioredoxin and treated by two sequential proteolytic enzymes to obtain functional hepcidin, in low yield < 10% (Gagliardo *et al*., 2008). A similar procedure was used to clone and express camel hepcidin, which showed to be functionally equivalent to the human one in binding and inhibiting ferroportin, using mouse monocyte-macrophage cell line J774 treated with Fe-nitrilotriacetate (Boumaiza *et al*., 2015). Here we planned to fuse camel hepcidin with human ferritin H-chain to obtain a chimeric camel hepcidin-human ferritin H-chain subunit (HepcH).

Ferritin is a spherical protein complex formed by 24 subunits of H- and L-chains which stores up to 4,000 iron atoms as an oxidized mineral core (Arosio *et al*., 2009). It is probably the most used protein in bionanotechnology. This is due to its well-known structural features, high stability, capability to mineralize metals in its cavity, self-assembly and possibility to redesign its interior and exterior by protein engineering (Martsev *et al*., 1998; Kanekiyo *et al*., 2013; Jutz *et al*., 2015). It has been used to encapsulate molecules, for the synthesis of inorganic cores, for functional nanostructured composite material, for magnetic nanoparticles with MRI applications and for carrying various epitopes (Cai *et al*., 2015). Most studies used the human H or L ferritin chains, which are able to self-assemble in different proportions to

produce a variety of heteropolymers (Santambrogio *et al*., 1993; Rucker *et al*., 1997). This allows the possibility to decorate ferritin surface with multiple functionalities through genetic and chemical modification to achieve desired properties for therapeutic and/or diagnostic purposes (Jeon *et al*., 2013). In particular, it can be used as peptide carrier that can target specific receptors.

In the present study, we describe an approach to produce and purify a chimeric camel hepcidin-human ferritin H-chain fusion protein (HepcH) that can be renatured onto a stable 24-mer ferritin shell when co-assembled together with human H- and L-chains. In addition, we demonstrate that the resulting assembled hybrid HepcH-FTH or -FTL is able to target the iron exporter ferroportin inducing its cellular internalization.

## Materials and Methods

*Plasmid construction*

The construct that overproduces HepcH monomer in *E.coli* was done in the pASK-IBA43plus vector (IBA, BioTAGnology). The first step was the insertion of the full human FTH cDNA, amplified by PCR using the primers NheI hFTH F / BamHI hFTH R (Table S1), in the NheI and BamHI sites. The second step was the insertion of camel hepcidin coding region cDNA, amplified by PCR using the primers NheI H25 F / NheI H25 R (Table S1), in the NheI site at the 5'end of huFTH sequence. The construct was verified by DNA sequencing, using the primers pASK F / pASK R (Table S1), which confirmed that the sequence of camel hepcidin-human ferritin H-chain was correct.

*Expression and solubilization of HepcH monomer*

Human ferritin H-chain fused directly downstream the mature camel hepcidin was cloned into the pASK-43 plus vector and expressed using BL21 (DE3) pLys *E. coli* strain. Growth of the transformed *E. coli* was done in 1 L LB medium (10 g Tryptone, 5 g Yeast extract, 5 g NaCl), with 100 µg/mL ampicillin, at 37°C, for 1-2 h until the culture reached an optical density ($OD_{600}$) of 0.5. Then the expression was induced by the addition of anhydrotetracycline with a final concentration of 200 µg/L, for 4 h. Cells were harvested by centrifugation at 7,000 RPM for 10 min. The pellet was washed twice in Tris-HCl 20 mM pH 7.4 and sonicated for cytoplasmic protein extraction. The sonicate pellet was then collected at 12,000 RPM and

washed twice in Tris 20 mM, 2 M Urea, 0.1% Triton X100, pH 7.4. The insoluble HepcH monomer was solubilized with a weight to volume ratio of 1:1 in 6 M Guanidine hydrochloride (GdnHCl) pH 4.7 and incubated with stirring for 18 h at 4°C. The suspension was sonicated to homogenize the solution.

*HepcH construct is expressed in association with iron*

Iron content in HepcH construct was determined by ferrozine assay. Briefly, the solubilized HepcH construct (4.5 μM) was incubated with 1 mM TCEP (Tris(2-carboxyethyl)phosphine hydrochloride, Sigma) in the presence of an excess of ferrozine (3-(2-Pyridyl)-5,6-diphenyl-1,2,4-triazine-p,p′-disulfonic acid monosodium salt hydrate, Sigma) in 50 mM Tris-HCl buffer pH 7.0. The rate of Fe(II) release was monitored by reading at 562 nm the formation of the ($[Fe^{II}(fz)_3]$) complex ($\varepsilon_{562}$= 28,000 $M^{-1}$ $cm^{-1}$). In parallel, a control containing HepcH construct (4.5 μM) and ferrozine, in absence of TCEP, was also monitored at 562 nm. Absorbance measurements were recorded using a Cary 50 Bio UV-vis spectrophotometer.

*Thiol quantification*

Thiol quantification of HepcH monomer was done using Ellman's method (Ellman, 1959). Briefly, the solubilized HepcH monomer (0.12 mg/mL, 5 μM) was first fully reduced by incubation with a molar excess of TCEP (tris(2-carboxyethyl)phosphine, Sigma) at 4ºC. After 1 h of incubation, the pH was lowered to 3.5-4 by drop-wise addition of 0.1 N HCl to inhibit disulfide bond formation, and the excess of unreacted TCEP was removed by successive dialysis steps at pH 4 using a 12 kDa dialysis membrane (Sigma). Free sulfhydryl quantification was then performed by incubation for 1 hour at room temperature with an excess of DTNB (5,5'-Dithio-bis-(2-nitrobenzoic acid), Sigma) at a final concentration of 500 μM in a reaction buffer containing 0.1 M sodium phosphate, 1 mM EDTA at pH 8. The total concentration of free thiol groups was measured spectrophotometrically at 412 nm using a value of 14,150 $M^{-1}$ $cm^{-1}$ for the molar extinction coefficient of $TNB^{2-}$. For free sulfhydryl-group detection in the final renatured HepcH-FTH and HepcH–FTL samples, we used the protocol described above without the reductive step with TCEP.

*Assembly of HepcH-FT heteropolymers*

Assembly of HepcH in an heteropolymeric molecule was performed by adding denatured FTH or FTL before renaturation, followed by 10-fold dilution in buffer. Prior to the refolding,

the HepcH monomer was made iron-free following the protocol described by Levi et al. with slight modifications (Levi *et al*., 1988). Briefly, solubilized HepcH monomer in 6 M GdnHCl was incubated with 1% thioglycolic acid, pH 5.5, and 2,2-bipyridyle followed by 48 h extensive dialysis against 6 M GdnHCl, pH 7.0. Once iron-free, the resulting clear colorless and unfolded HepcH sample was incubated with different ratios of FTH or FTL denatured in 6 M or 8 M GdnHCl respectively, at pH 3.5, using different HepcH/FT molar ratios (5:1; 1:1; 1:2; 1:5; 1:11). The mixture was then refolded by at least 10-fold dilution into 0.1 M Tris-HCl buffer pH 7.4, 2 mM TCEP, and then incubated at 4°C for 1-2 days. The resulting solution was then clarified by centrifugation at 4,000 RPM for 15 min, concentrated 10-fold using a 100 kDa molecular weight cut-off centrifugal filter (Millipore, Billerica, Massachusetts) and analyzed in 7% non-denaturing PAGE. Cysteine oxidation for the final refolded HepcH-FTH and HepcH-FTL heteropolymers renatured in the proportions 1:2; 1:5 and 1:11, was carried out using the glutathione redox system (GSH/GSSG) as described by Jordan et al. (Jordan *et al*., 2009). Briefly, the refolded hybrid ferritin samples containing HepcH construct were dialyzed for 48 h at 4ºC using a 12 kDa dialysis membrane (Sigma) against a buffer containing 0.1 M Tris pH 8 and 0.4 mM GSH/ 0.4 mM GSSG in order to slowly oxidize cysteine thiols in parallel with gradual removal of the TCEP, enhancing thus the intramolecular S-S formation. Then the sample was thoroughly dialyzed at room temperature against 20 mM Tris-HCl pH 7.4 to remove the GSG/GSSG redox system and the resulting oxidized HepcH-FTH and -FTL were run on a native 7% PAGE. Sample concentration was measured with Bradford assay (Biorad) using BSA as a control.

*Western blot analysis*

Samples of 30 µg of protein were loaded on 12% SDS-PAGE or 7% non-denaturing PAGE and then blotted onto Amersham Western blotting membrane (GE Healthcare, Life Sciences) with monoclonal anti-human FTH and FTL (Sigma Aldrich) and polyclonal anti-hepcidin (Rabbit anti-hepcidin-25, Abcam) antibodies for SDS-PAGE. For non-denaturating PAGE, monoclonal antibodies rH02 and LF03, prepared against human ferritin H- and L-chains respectively, were used as previously described (Luzzago *et al*., 1986; Cozzi *et al*., 1989). Briefly, the membrane was blocked with 2% defatted milk in TBS-T for 30 min at 37°C under agitation and then incubated with anti-human FTH or FTL (1:1,000) and anti-hepcidin (1:1,000) primary antibodies during 1-2 h at 37°C or overnight at 4°C. After washing 3 times with TBS-T, the membrane was incubated for 1 h at 37°C with the secondary anti-mouse

(1:20,000) and then with anti-rabbit (1:15,000) antibodies conjugated with peroxidase (anti-mouse immunoglobulin G, Dako or anti-rabbit immunoglobulin G, BioFX Laboratories). After washing 3 times at room temperature the signal was revealed by enhanced chemiluminescence (ECL) kit (GE, Healthcare) and recorded with KODAK Image Station 440CF (Kodak).

*Matrix-Assisted Laser Desorption/Ionization (MALDI) Time-of-Flight (TOF)/TOF Mass Spectrometry (MS) [MALDI-TOF/TOF–MS] analysis*

MALDI-TOF/TOF–MS analysis was performed on AB Sciex 5800 MALDI-TOF/TOF–MS as described by Gianoncelli and coworkers (Gianoncelli *et al*., 2015).

*Cellular studies*

Mouse monocyte-macrophage cell line J774 (Lombardy and Emilia Romagna Experimental Zootechnic Institute) was cultured as previously described (Delaby *et al*., 2005). Briefly, cells were grown in DMEM (PAA Laboratories GmbH), 10% endotoxin-free fetal bovine serum (Euroclone), 0.04 mg/mL gentamicin (Euroclone), 2 mM L-glutamine (PAA Laboratories GmbH), and maintained at 37°C in 5% $CO_2$. Cells (200,000 cells/well) were seeded onto 12-well plates, and after 24 h were grown for 12 h in presence of 100 μM ferric ammonium citrate (FAC) to induce ferroportin expression. The day after, cells were incubated with the hybrid ferritin heteropolymers containing different ratio of HepcH:FTH at a final concentrations of 0.2 μM (1:5) and 0.2 μM (1:11) and HepcH:FTL at a final concentrations of 0.1 μM (1:5) and 0.2 μM (1:11). The controls were cells without FAC treatment and the native FTH and FTL homopolymers at the same concentrations. Experiments were done at 37°C for 15, 30, 60 and 120 minutes. After this time, the supernatant was discarded and the cells washed with cold PBS and lysed using cold buffer (200 mM Tris-HCl at pH 8, 100 mM NaCl, 1 mM EDTA, 0.5% NP-40, 10% glycerol, 1 mM sodium fluoride, 1 mM sodium orthovanadate, Protease Inhibitor Cocktail; Roche). Protein content was determined by colorimetric BCA assay (bicinchoninic acid assay, Pierce) and 20 μg of total proteins were separated by native polyacrylamide gel electrophoresis and Western Blotting was performed using polyclonal anti-rabbit ferroportin, anti-human FTH (RH02) and FTL (LF03) antibodies for the detection of proteins internalized by the cells.

## Results

157 *Chimeric construct for HepcH expression*

158 The HepcH plasmid construct encoding the sequence of the mature camel hepcidin fused to
159 that of the human H ferritin (huFTH) is shown in Fig. 1A. In the ferritin shell the N-terminus
160 of the subunits is exposed, thus the fused hepcidin is expected to be accessible and available
161 for ferroportin binding. The HepcH monomer of 213 amino acids (Fig. 1A and Table I) was
162 efficiently expressed by the transformed *E. coli* and it had the expected molecular size of 24
163 kDa on SDS-PAGE (Fig. 1B). In immunoblotting experiments, the HepcH monomer was
164 recognized by antibodies specific for human FTH and for hepcidin-25, which also recognized
165 the recombinant FTH and the commercial human Hepcidin-25, respectively (Fig. 1C). In
166 MALDI-TOF mass spectrometry, HepcH monomer solubilized in 6 M GdnHCl pH 4.7,
167 exhibited a peak at m/z 24339.55 corresponding to the theoretical average mass of 24410.50
168 (Fig. 1D and Table I). The peak at m/z 48466.0313 corresponds to HepcH dimer (Fig. 1D).

169 *The insoluble HepcH is expressed in association with iron*

170 The insoluble fractions of the homogenate of cell expressing HepcH subunit showed a distinct
171 reddish color not present in those expressing huFTH (Fig. 2A). Treatments of the precipitates
172 with 6 M urea at pH 4.5–5.0 solubilized the recombinant protein together with the color (Fig.
173 2A). The UV/Vis absorption spectra of solubilized HepcH subunit showed a major peak at
174 280 nm and a shoulder around 420 nm (Fig. 2B, black line) not present in ferritin H-chain
175 (Fig. 2B, grey line) that decreased after reduction with 100 mM dithionite (Fig. 2B, dashed
176 line). A similar behavior was described for a FTH-Hepcidin chimera expressed in *E.coli* in
177 association with iron (Gerardi *et al*., 2005). The iron bound to HepcH was quantified amounts
178 by chelation with ferrozine. The solubilized preparation was incubated with ferrozine and an
179 agent (TCEP) to reduce iron, and the formation of the ($[Fe^{II}(fz)_3]$) complex was followed by
180 its absorbance at 562 nm. The colorimetric reaction started immediately after addition of
181 TCEP and reached a plateau after 24 hours (Fig. 2C). In the absence of reducing agent, the
182 color development was negligible (Fig. 2D) indicating that the bound iron is the Fe(III) form.
183 We calculated a value of ~19 μM of iron in the complex, corresponding to about 4.1 Fe atoms
184 per HepcH monomer, as isolated.

185 *Quantification of free sulfhydryl groups in the solubilized HepcH*

186 FTH has 3 Cys and hepcidin has 8, thus the detection of the free thiols was of interest. The
187 purified HepcH peptide was subjected to Ellman's assay. The absorbance spectra of HepcH

incubated with 500 μM of DTNB before and after reduction of the thiols are shown in Fig. S1. We calculated ~38.7 μM of sulfhydryl groups in the HepcH sample after full reduction corresponding to about 7.7 free sulfhydryl per HepcH monomer (Fig. S1, bars). This indicates that all the thiols are not accessible under non-reducing conditions, and that after reduction about 8 out of 11 become accessible, confirming the presence of the hepcidin extension in the purified HepcH construct.

*Assembly, oxidation and characterization of HepcH-FTH and HepcH-FTL heteropolymers*

Initial experiments to renature HepcH by diluting the denatured peptide into the renaturing buffers as in (Santambrogio *et al*., 1993) were unsuccessful, indicating that the N-terminal hepcidin interferes with folding or assembly. Thus, we tried the co-renaturation together with H- or L-chains, on the basis of previous evidence that co-assembly facilitates the folding of altered ferritin chains (Levi *et al*., 1994). We set up a series of experiments in which the denatured and reduced HepcH was firstly mixed with denatured FTH or FTL at different ratios, and then refolded by 10-fold dilution in buffer to test the formation of stable ferritin shells. We obtained heteropolymeric ferritins composed of HepcH and FTH or FTL only when mixed in the proportions 1:11; 1:5 and in a less extent in 1:2. The assembled ferritin shells produced a single discrete band in 8% non-denaturing PAGE, the mobility of which decreased with the increase of HepcH, an indirect support that the hepcidin moiety is exposed and slows the mobility (Fig. 3A and 3B). When the refolding was done with higher proportions of HepcH:FT (1:1, 2:1 and 5:1), the product showed a large smear on PAGE indicating the formation of disordered and poorly structured molecules (Fig. 3A). Immunoblotting with anti-human FTH and anti-hepcidin antibodies, confirmed the presence of HepcH construct assembled in ferritin shells (Fig. 3C). A schematic representation of the renatured HepcH-FT hybrid heteropolymer is shown in the Fig. 3D. Renaturation of the hybrid ferritins was done under reducing conditions, and thus needed the re-oxidation of the hepcidin cysteines to form the four disulfide bridges present in hepcidin structure. For this reason, the hybrid ferritins were incubated with the glutathione redox system at pH 8 to promote formation of thiosulfate anions, which represent the reactive species during disulfide formation. The redox pair consisted of reduced and oxidized glutathione at concentrations of 0.4 mM each, followed by extensive dialysis. The final oxidized heteropolymeric HepcH-FTH and HepcH-FTL showed the typical ferritin monomer and oligomers ladder pattern in PAGE (Fig. 4A) and no free thiols could be detected by Ellman's reaction testifying the full oxidation of the eight cysteine residues constituting the camel hepcidin (Fig. 4B, bars).

MALDI-TOF spectra of the final oxidized HepcH-FTH heteropolymer exhibited, average mass peaks at m/z 21,296.84 and at 24,338.90 (Fig. S2 A and Table I) which corresponds to the theoretical average mass $[M+H]^+$ of 21,225.64 of FTH (183 amino acids), and of 24,410.50 to HepcH (213 amino acids). The HepcH-FTL showed a peak at 20,055.41 and at 24,230.14, the former corresponding to the 20,019.67 of FTL (175 amino acids) monomers (Fig. S2 and Table I). The differences between the theoretical and experimental masses is due to the instrument settings that for mid/high MW uses only one time of flight and has low resolution with deviations up to 100 Da.

*The HepcH-FTH heteropolymers bind macrophagic cells and cause ferroportin degradation*

The major hepcidin function is to bind ferroportin exposed to cellular plasma membrane an activity that we expected could be monitored by taking advantage of the ferritin bound to it. To verify this, we incubated the mouse macrophage J774 cell with 100 μM FAC to induce ferroportin expression, the cells were incubated with the heteropolymers using FTH and FTL homopolymers as controls. Immunoblotting with anti-ferritin antibodies showed that HepcH-FTH and FTL were strongly retained by the cells after 2h of incubation using the molar ratio HepcH/FT of 1:5 (Fig. 5A and 5B). However, 15-30min of cell treatment was insufficient for the binding of this ferritins on the macrophage cell surface (data not shown). Moreover, the FTH and FTL homopolymers were retained only in trace amounts after 2h of incubation (Fig. 5A and 5B). Interestingly, the intensity of the binding increased with the increase of the proportion of HepcH in the heteropolymers, both with FTH and FTL (Fig. 5A and 5B, ratio 1:5 versus 1:11). This indicates that the binding can be safely attributed to the exposed hepcidin moiety that likely interacts with ferroportin. After binding, the hepcidin role is to induce ferroportin degradation, therefore to verify this we analyzed the ferroportin content of the treated cells by western blotting using anti-ferroportin antibodies. Figure 5C shows that the recombinant heteropolymer HepcH-FTH induced a degradation of ferroportin similar to that by treatment with synthetic hepcidin and higher than untreated cells and cells treated with native ferritin.

## Discussion

The production of a functional hepcidin attached to a large multimeric protein like ferritin may be useful to follow hepcidin binding to ferroportin and analyze its functionality. In a

previous approach, we fused the hepcidin moiety at the C-terminus of ferritin, but the hepcidin was buried inside the cavity and thus not functional (Gerardi *et al*., 2005). Here we succeed to fuse at the N-terminus of the ferritin H-chain a camel hepcidin, which differs from the human one in only 2 residues and is similarly functional and more stable (Boumaiza *et al*., 2014, 2015). This strategy was expected to display the N-terminal domain of hepcidin exposed and available to the interaction with ferroportin (Nemeth *et al*., 2005; Preza *et al*., 2011). The HepcH construct was efficiently expressed in *E. coli* as insoluble reddish aggregate rich in iron. The approaches to renature the construct were unsuccessful, indicating that the hepcidin moiety interferes with the process of ferritin folding and assembly. This did not occur when hepcidin was fused at the C-terminus and formed soluble and stable ferritin shells (Gerardi *et al*., 2005). A common property of the two chimeric constructs is the binding of iron during expression in *E. coli*, which in the present study was calculated to be about 4 iron atoms per hepcidin molecule. The spectroscopic characteristics of the HepcH construct as isolated were reminiscent to the ones of Fe/S clusters. Its UV/vis spectrum showed a broad shoulder at 420 nm, which was absent in the wild-type ferritin. This is very likely due to the Cys dense sequence of hepcidin that may form active iron binding sites under low potential conditions. In fact, we found that the thiols of these Cys were not available if not treated with reducing agents. The insolubility of the HepcH was initially attributed to the Cys-iron complexes, but also the approaches to renature it under reducing conditions failed, indicating that the hepcidin moiety interferes with the folding/assembly. To solve this problem, we took advantage of the capacity of ferritin subunits to co/assemble together and facilitate their folding. For example, an insoluble L-chain with ferroxidase activity was induced to fold and assemble together with wild type L-chain (Levi *et al*., 1994). This approach worked also in this situation and we obtained heteropolymers of HepcH with both the H- and L-chains. We tried different HepcH:FTH and HepcH:FTL molar ratios, and we obtained a maximum number of about 4 HepcH subunits per shell (ratio 1:5). When HepcH was in excess, the renaturation was not successful. The ferritins so obtained retained all the characteristics of hybrid molecules, including the electrophoretic mobility and the recognition by antibodies for the two moieties, ferritin and hepcidin. Of interest is that disulfide bridges are not involved in wild-type ferritin stability, and thus the hybrid ferritin shells could be treated with glutathione redox system to allow the proper formation of the hepcidin disulfides bonds. This was apparently successful, since after the treatments no thiol group was accessible to Ellman's reagent, and, more important, the heteropolymers was able to bind J774 cells exposing ferroportin. The specificity of the binding to the cells was indicated by the evidence that it

occurred only with the HepcH-containing molecules and that its strength was related to the HepcH content. A minor binding was found with FTH homopolymers, probably due to the expression of the H-ferritin receptor TIM-2 in these cells (Han *et al*., 2011), while the binding of the FTL homopolymer was negligible. Hepcidin exerts it function by binding and then inducing ferroportin degradation, and in fact we observed that after 2 h incubation with HepcH-FTH the level of ferroportin in the J774 cells decreased, as it occurred in the cells treated with the synthetic hepcidin, while the incubation with FTH had no evident effect. This indicates that heteropolymer is biologically functional.

In conclusion, present data show a genetic approach to produce hepcidin displayed on ferritin surface. Fusion hepcidin-ferritin H subunit assembled together with H- or L-chains at a ratio of 1:5, produced a stable and functional 24-mer ferritin exposing about 4 hepcidin per shell. The evidence that this molecule specifically binds cells that express high levels of ferroportin indicates that it might be an interesting tool to study more in detail the mechanism of interaction of hepcidin and ferroportin and how the complex is degraded. It might also be used as an alternative approach for the development of new concepts and prodrugs of anticancer drug-vectorization using the specific hepcidin-ferroportin cell internalization pathway.

## Acknowledgements

Special thanks for the technical help of Dr Magdalena Gryzik at the Department of Molecular and Translational Medicine, University of Brescia, Viale Europa 11, Brescia, Italy. Dr Mohamed Boumaiza was supported by a fellowship from “Consorzio Interuniversitario Biotecnologie” of Italy. This work is partially financed by the Laboratory of Protein Engineering and Bioactive Molecules (LIP-MB) and the Doctoral School of the National Institute of Applied Sciences and Technology (INSAT-Tunis)-University of Carthage.

## References

Arosio,P., Ingrassia,R. and Cavadini,P. (2009) *Biochim. Biophys. Acta.*, **1790**, 589–599.

Blanchette,N.L., Manz,D.H., Torti,F.M. and Torti,S.V. (2016) *Expert Rev. Hematol.*, **9**, 169–86.

316 Boumaiza,M., Ezzine,A., Jaouen,M., Sari,M.A. and Marzouki,M.N. (2014) *J. Pep. Sci*., **20**,
317 680–688.
318 Boumaiza,M., Jaouen,M., Deschemin,J.C., Ezzine,A., Khalaf,N.B., Vaulont,S.,
319 Marzouki,M.N. and Sari,M.A. (2015) *Protein Expr. Purif*., doi:
320 http://dx.doi.org/10.1016/j.pep.2015.04.016.
321 Cai,Y., Cao,C., He,X., Yang,C., Tian,L., Zhu,R. and Pan,Y. (2015) *Int. J. Nanomedicine*, **10**,
322 2619–2634.
323 Cozzi,A., Levi,S., Bazzigaluppi,E., Ruggeri,G. and Arosio,P. (1989) *Clin. Chim. Acta*, **184**,
324 197–206.
325 Delaby,C., Pilard,N., Gonçalves,A.S., Beaumont,C., and Canonne,H.F. (2005) *Blood*, **106**,
326 3979–3984.
327 Ellman,G.L. (1959) *Arch. Biochem. Biophys.*, **82**, 70–7.
328 Falzacappa,M.V. and Muckenthaler,M.U. (2005) *Gene*, **364**, 37–44.
329 Gagliardo,B., Faye,A., Jaouen,M., Deschemin,J.C., Cannone-Hergaux,J.F., Vaulont,S. and
330 Sari,M.A. (2008) *FEBS J*., **275**, 3793–3803.
331 Ganz,T. (2003) *Blood*, **102**, 783–788.
332 Gerardi,G., Biasiotto,G., Santambrogio,P., Zanella,I., Ingrassia,R., Corrado,M, Cavadini,P.,
333 Derosas,M.. Levi,S. and Arosio,P. (2005) *Blood Cells Mol. Dis.*, **35**, 177–181.
334 Gianoncelli,A., Bonini,S.A., Bertuzzi,M., Guarienti,M., Vezzoli,S., Kumar,R., Delbarba,A.,
335 Mastinu,A., Sigala,S., Spano,P. *et al*. (2015) *BioDrugs*, **29**, 285–300.
336 Han,J., Seaman,W.E., Di,X., Wang,W, Willingham,M., Torti,F.M. and Torti,S.V. (2011)
337 *PLoS ONE*, doi: 10.1371/journal.pone.0023800.
338 Houamel,D., Ducrot,N., Lefebvre,T., Daher,R., Moulouel,B., Sari,M.A., Letteron,P.,
339 Lyoumi,S., Millot,S., Tourret,J. *et al.* (2016) *J. Am. Soc. Nephrol*., **27**, 835–46.
340 Jeon,J.O., Kim,S., Choi,E., Shin,K., Cha,K., So,I.S., Kim,S.J., Jun,E. Kim,D. and Ahn,H.J.
341 (2013) *ACS NANO*, **7**, 7462–7471.
342 Jordan,J.B., Poppe,L., Haniu,M., Arvedson,T., Syed,R., Li,V., Kohno,H., Kim,H.,
343 Schnier,P.D. Harvey,T.S. *et al.* (2009) *J. Biol. Chem.*, **284**, 24155–24167.
344 Jutz,G., van Rijn,P., Miranda,B.S. and Böker,A. (2015) *Chem. Rev.*, **115**, 1653–701.
345 Kanekiyo,M., Wei,C.J., Yassine,H.M., McTamney,P.M., Boyington,J.C., Whittle,J.R.R.,
346 Rao,S.S., Kong,W.P., Wang,L. and Nabel,G.J. (2013) *Nature*, doi:10.1038/nature12202.
347 Krause,A., Neitz,S., Magert,H.J., Schulz,A., Forssmann,W.G., Schulz,K.P. and Adermann,K.
348 (2000) *FEBS let*., **480**, 147–50.

Lehtihet,M., Bonde,Y., Beckman,L., Berinder,K., Hoybye,C., Rudling,M., Sloan,J.H., Konrad,R.J., and Angelin,B. (2016) *PLoS ONE*, doi:10.1371/journal.pone.0148802.

Levi,S., Corsi,B., Rovida,E., Cozzi,A., Santambrogio,P., Albertini,A., and Arosio,P. (1994) *J. Biol. Chem.*, **269**, 30334–30339.

Levi,S., Luzzago,A., Cesareni,G., Cozzi,A., Franceschinelli,F., Albertini,A. and Arosio,P. (1988) *J. Biol. Chem.*, **263**, 18086–18092.

Luzzago,A., Arosio,P., Iacobello,C., Ruggeri,G., Capucci,L., Brocchi,E., Simone,F.D., Gamba,D., Gabri,E., Levi,S. *et al*. (1986) *Biochim. Biophys. Acta*, **872**, 61–71.

Martsev,S.P., Vlasov,A.P., and Arosio,P. (1998) *Protein Eng*., **11**, 377–381.

Nemeth,E. and Ganz,T. (2006) *Annu. Rev. Nutr*., **26**, 323–342.

Nemeth,E., Preza,G.C., Jung,C.L., Kaplan,J., Waring,A.J. and Ganz,T. (2005) *Blood*, **107**, 328–33.

Pantopoulos,K., Porwal,S.K., Tartakoff,A. and Devireddy,L. (2012) *Biochemistry*, **51**, 5705–5724.

Park,C.H., Valore,E.V., Waring,A.J. and Ganz,T. (2001) *J. Biol. Chem.*, **276**, 7806–7810.

Preza,G.C., Ruchala,P., Pinon,R., Ramos,E., Qiao,B., Peralta,M.A., Sharma,S., Waring,A., Ganz,T., Nemeth,E. (2011) *J. Clin. Invest.*, **121**, 4880–4888.

Ramey,G., Deschemin,J.C., Durel,B., Hergaux,F.C., Nicolas,G. and Vaulont,S. (2010) *Haematologica*, **95**, 501–504.

Recalcati,S., Minotti,G. and Cairo,G. (2010) *Antioxid. Redox Signal.*, doi: 10.1089 /ars.2009.2983.

Rucker,P., Torti,F.M., and Torti,S.V. (1997) *Protein Eng*., **10**, 967–973.

Santambrogio,P., Levi,S., Cozzi,A., Rovida,E., Albertini,A. and Arosio,P (1993) *J. Biol. Chem.*, **268**, 12744–8.

## Figure legends

### Figure 1. Expression and analysis of the HepcH chimeric construct.

A: amino acid sequence of the HepcH monomer (camel hepcidin sequence in red; human ferritin H sequence in blue). B: SDS-PAGE analysis of the induced and non-induced *E.coli* transformed by the recombinant HepcH pASK-IBA 43 plus vector. Lane 1 and 2, induced and non-induced pellet respectively (insoluble fraction). Lane 3 and 4, induced and non-induced supernatant (soluble fraction). Lane 5 and 6, induced and non-induced total sonicate (total protein). C: Western blotting analysis of the denaturing PAGE of the recombinant HepcH monomer (2 different blots). Blot 1: lane 1, rabbit hepcidin antibodies recognized the commercial human hepcidin-25 (control). Lane 2, rabbit hepcidin antibodies recognized HepcH. Blot 2: lane 3, mouse rH02 antibodies recognized HepcH. Lane 4, mouse rH02 antibodies recognized the recombinant human H-ferritin, huFTH, (control). D: MALDI-TOF mass analysis of the recombinant HepcH monomer.

### Figure 2. Iron is bound to the insoluble HepcH.

A: The insoluble fraction of the *E.coli* expressing HepcH had a reddish color (left) distinct from the light brown color (at the right) of *E. coli* expressing huFTH. B: UV/Vis spectra of the two fractions solubilized in 5 M urea (0.5 mg/ml proteins) before and after incubation with 100 mM dithionite. C: UV-vis spectra of solubilized HepcH reduced with TCEP in the presence of ferrozine that readily chelates iron with the formation of the Fe(II)-ferrozine complex that absorbs at 562 nm. Inset: Absorbance at 562 nm plotted versus time shows the appearance of a plateau after 24 h of reaction. D: UV-vis spectra of HepcH monomer incubated with presence of ferrozine in absence of reducing agent. Inset: Absorbance at 562 nm plotted versus time.

### Figure 3. Assembly of HepcH-FTH and -FTL heteropolymers.

A: Non-denaturing PAGE analysis of the assembled HepcH-FTH obtained after mixing different ratios of denatured HepcH and FTH monomers. B: Non-denaturing PAGE analysis of the assembled heteropolymeric HepcH-FTH and HepcH-FTL at different ratios. C: Non-denaturing PAGE analysis and Western blotting of the refolded HepcH-FTH and –FTL heteropolymers, using monoclonal anti-human FTH and FTL and polyclonal anti-hepcidin-25

antibodies, indicating that HepcH assembles in ferritin shells. Indeed, refolding of the HepcH alone was impossible due to hepcidin aggregates. D: Schematic representation of the possible geometries of the renatured HepcH-FT hybrid heteropolymer. Yellow star corresponds to the HepcH monomer. Ratio HepcH / FTH or FTL = 1:1, corresponding to average number of 12 HepcH per 24 subunits. Ratio HepcH / FTH or FTL =1:2, corresponding to average number of 8 HepcH per 24 subunits. Ratio HepcH / FTH or FTL =1:5, corresponding to average number of 4 HepcH per 24 subunits. Ratio HepcH / FTH or FTL =1:11, corresponding to average number of 2 HepcH per 24 subunits.

**Figure 4. Characterization of cysteine oxidized heteropolymers.**

A: Non-denaturing PAGE analysis of the assembled heteropolymeric HepcH-FTH and HepcH-FTL heteropolymers after cysteine oxidation. Refolded native FTH and FTL were used as control. B Left: UV-vis spectra of Ellman's assay of the final oxidized heteropolymeric HepcH-FTH (dashed) and HepcH-FTL (dots) at 1:5 ratios showing the absence of absorption bands at 412 nm. B Right: thiol quantification of HepcH-FTH (white column) and HepcH-FTL (black column) expressed as number of free sulfhydryl groups per HepcH moiety in the final heteropolymeric 24-mers, considering a number of 4 HepcH per shell.

**Figure 5. HepcH-FTH heteropolymers bind iron treated J774 cells and cause ferroportin degradation**. A: Western blotting analysis of the non-denaturing PAGE of cell lysates after treatment with 0.2 μM HepcH-FTH (1:5 and 1:11) during 1 h and 2 h incubation using monoclonal anti-human FTH antibody. B: Western blotting analysis of the non-denaturing PAGE of cell lysates after treatment with 0.1 μM and 0.2 μM HepcH-FTL (1:5 and 1:11) during 1 h and 2 h incubation using monoclonal anti-human FTL antibody. Controls containing 0.2μM of native huFTH, and 0.1 μM and 0.2 μM of native huFTL were incubated at same final volumes and same reaction times with cells. NT, non-treated cells used as control. C: Western blotting analysis of the SDS-PAGE of cell lysates using polyclonal anti-rabbit ferroportin antibody. CTR: untreated cells. FTH: cells treatment with 0.5 μM native FTH for 2 h. HepcH-FTH: cells treatment with 0.2 μM HepcH-FTH (1:5) for 2 h. Hepc: cells treatment with 0.5 μM synthetic human hepcidin-25 for 2 h. Non-adjacent bands, from the same blot, were denoted by vertical black lines.

## Tables

**Table I.** Mass measurements of the recombinant ferritin subunits before and after renaturation and oxidation.

| **Name** | AA | Theoretical monoisotopic mass $[M+H]^+$ | Theoretical average mass $[M+H]^+$ | Experimental $[M+H]^+$ (in 6M GdnHCl) | Experimental $[M+H]^+$ (after ferritin recovering and cysteine oxidation) |
|---|---|---|---|---|---|
| **HepcH** | 213 | 24,394.53 | 24,410.50 | 24,339.55* | 24,338.90 *<br>24,230.14 * |
| **FTL** | 175 | 20,007.10 | 20,019.67 | -- | 20,055.41 * |
| **FTH** | 183 | 21,212.29 | 21,225.64 | -- | 21,296.84* |

* average mass

447

448 **Supplementary data**

449 **Table S1. Primers used in this study.**

450 **Figure S1. Thiol quantification on the solubilized HepcH monomer.**

451 A: UV-vis spectra showing the results of Ellman's assay for thiol detection in the solubilized
452 HepcH monomer (dashed) and the HepcH monomer subjected to reductive treatment (black
453 line). Spectra show the appearance of an absorption band at 412 nm after reductive treatment
454 in HepcH revealing the presence of cysteine sulfhydryl-groups. B: Amount of free sulfhydryl-
455 groups per HepcH present in HepcH after reduction (black) and in the solubilized HepcH
456 (white).

457 **Figure S2. MALDI-TOF spectra of the assembled HepcH-FTH (A) and -FTL (B)**
458 **heteropolymers (ratio 1:5).**

459

460

Figure 1

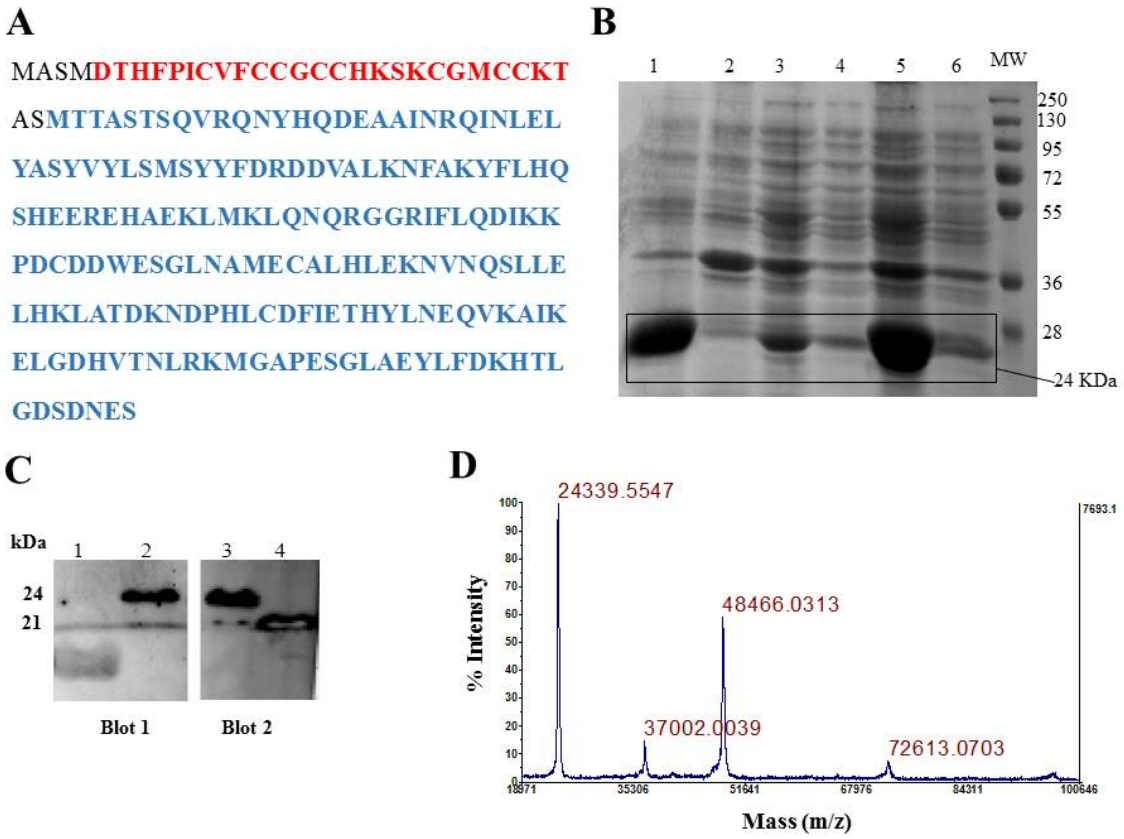


**Figure 1. Expression and analysis of the HepcH chimeric construct.**

A: amino acid sequence of the HepcH monomer (camel hepcidin sequence in red; human ferritin H sequence in blue). B: SDS-PAGE analysis of the induced and non-induced *E.coli* transformed by the recombinant HepcH pASK-IBA 43 plus vector. Lane 1 and 2, induced and non-induced pellet respectively (insoluble fraction). Lane 3 and 4, induced and non-induced supernatant (soluble fraction). Lane 5 and 6, induced and non-induced total sonicate (total protein). C: Western blotting analysis of the denaturing PAGE of the recombinant HepcH monomer (2 different blots). Blot 1: lane 1, rabbit hepcidin antibodies recognized the commercial human hepcidin-25 (control). Lane 2, rabbit hepcidin antibodies recognized HepcH. Blot 2: lane 3, mouse rH02 antibodies recognized HepcH. Lane 4, mouse rH02 antibodies recognized the recombinant human H-ferritin, huFTH, (control). D: MALDI-TOF mass analysis of the recombinant HepcH monomer.

Figure 2

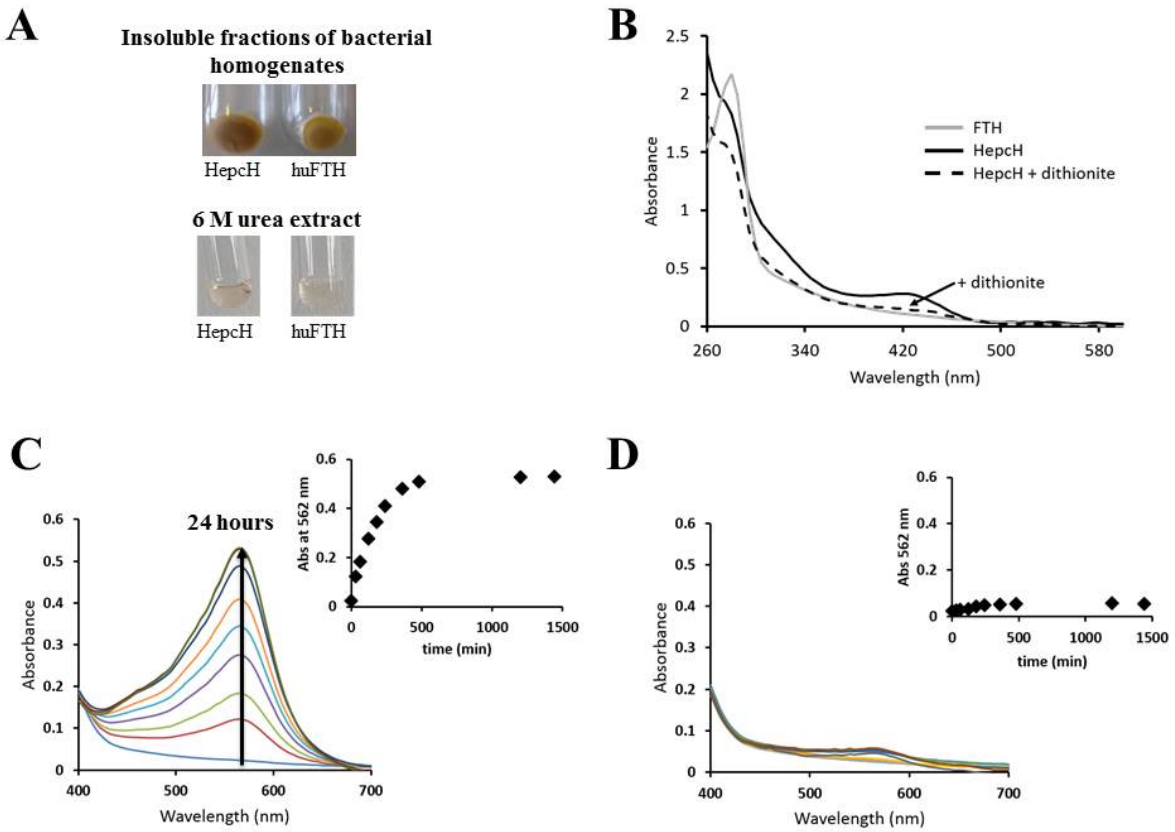


**Figure 2. Iron is bound to the insoluble HepcH.**

A: The insoluble fraction of the E.coli expressing HepcH had a reddish color (left) distinct from the light brown color (at the right) of E. coli expressing huFTH. B: UV/Vis spectra of the two fractions solubilized in 5 M urea (0.5 mg/ml proteins) before and after incubation with 100 mM dithionite. C: UV-vis spectra of solubilized HepcH incubated reduced with TCEP in the presence of ferrozine that readily chelates iron with the formation of the Fe(II)-ferrozine complex that absorbs at 562 nm. Inset: Absorbance at 562 nm plotted versus time shows the appearance of a plateau after 24 h of reaction. D: UV-vis spectra of HepcH monomer incubated with presence of ferrozine in absence of reducing agent. Inset: Absorbance at 562 nm plotted versus time.

Figure 3

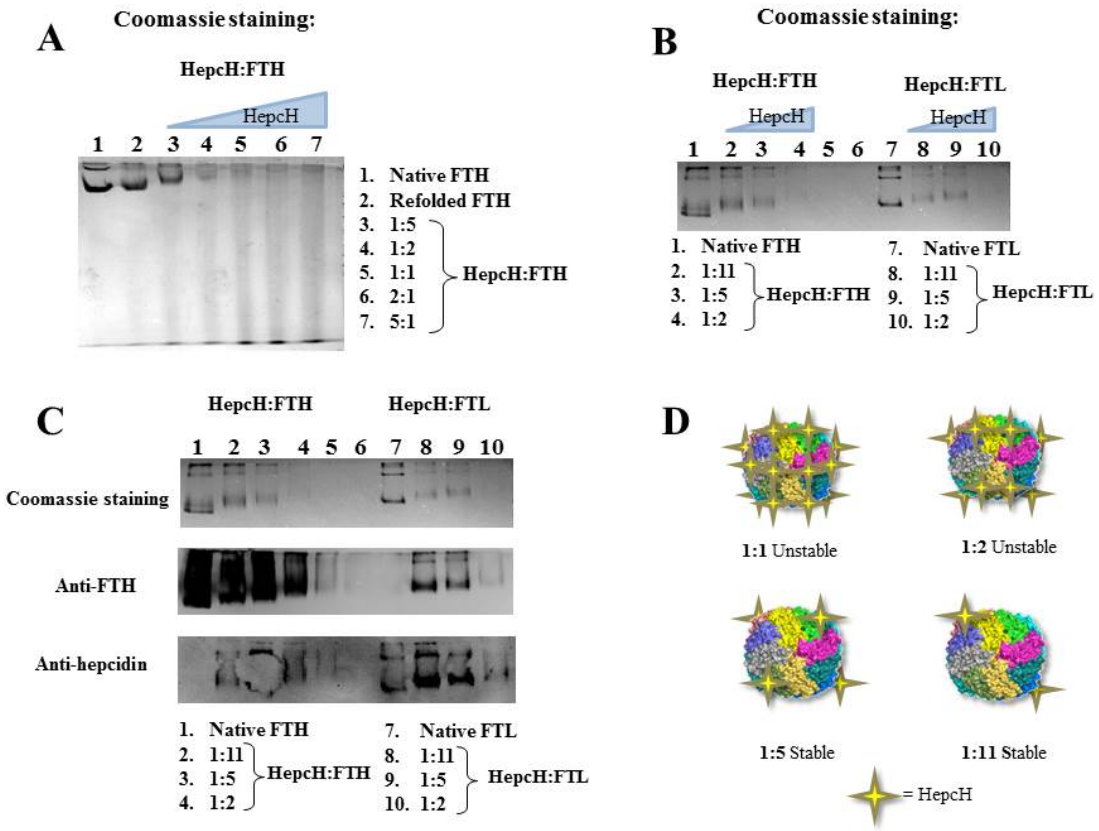


**Figure 3. Assembly of HepcH-FTH and -FTL heteropolymers.**

A: Non-denaturing PAGE analysis of the assembled HepcH-FTH obtained after mixing different ratios of denatured HepcH and FTH monomers. B: Non-denaturing PAGE analysis of the assembled heteropolymeric HepcH-FTH and HepcH-FTL at different ratios. C: Non-denaturing PAGE analysis and Western blotting of the refolded HepcH-FTH and –FTL heteropolymers, using monoclonal anti-human FTH and FTL and polyclonal anti-hepcidin-25 antibodies, indicating that HepcH assembles in ferritin shells. Indeed, refolding of the HepcH alone was impossible due to hepcidin aggregates. D: Schematic representation of the possible geometries of the renatured HepcH-FT hybrid heteropolymer. Yellow star corresponds to the HepcH monomer. Ratio HepcH / FTH or FTL = 1:1, corresponding to average number of 12 HepcH per 24 subunits. Ratio HepcH / FTH or FTL =1:2, corresponding to average number of 8 HepcH per 24 subunits. Ratio HepcH / FTH or FTL =1:5, corresponding to average number of 4 HepcH per 24 subunits. Ratio HepcH / FTH or FTL =1:11, corresponding to average number of 2 HepcH per 24 subunits.

Figure 4

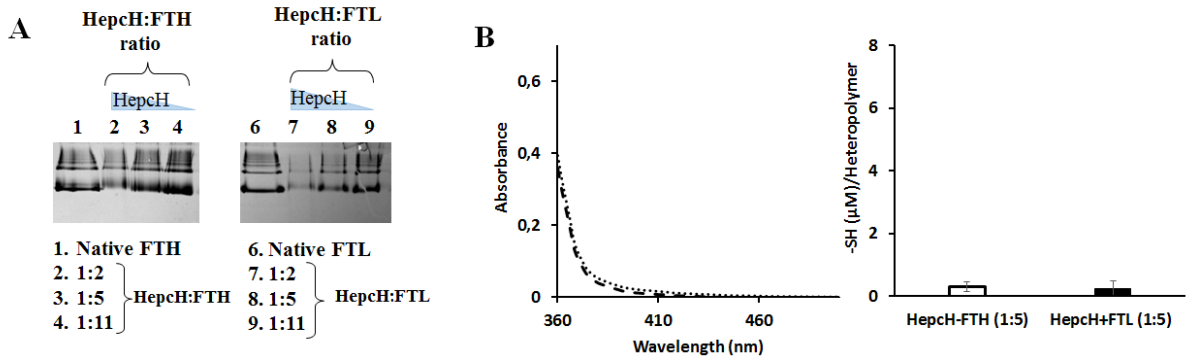


505

506 **Figure 4. Characterization of cysteine oxidized heteropolymers.**

507 A: Non-denaturing PAGE analysis of the assembled heteropolymeric HepcH-FTH and
508 HepcH-FTL heteropolymers after cysteine oxidation. Refolded native FTH and FTL were
509 used as control. B Left: UV-vis spectra of Ellman's assay of the final oxidized
510 heteropolymeric HepcH-FTH (dashed) and HepcH-FTL (dots) at 1:5 ratios showing the
511 absence of absorption bands at 412 nm. B Right: thiol quantification of HepcH-FTH (white
512 column) and HepcH-FTL (black column) expressed as number of free sulfhydryl groups per
513 HepcH moiety in the final heteropolymeric 24-mers, considering a number of 4 HepcH per
514 shell.

515

516

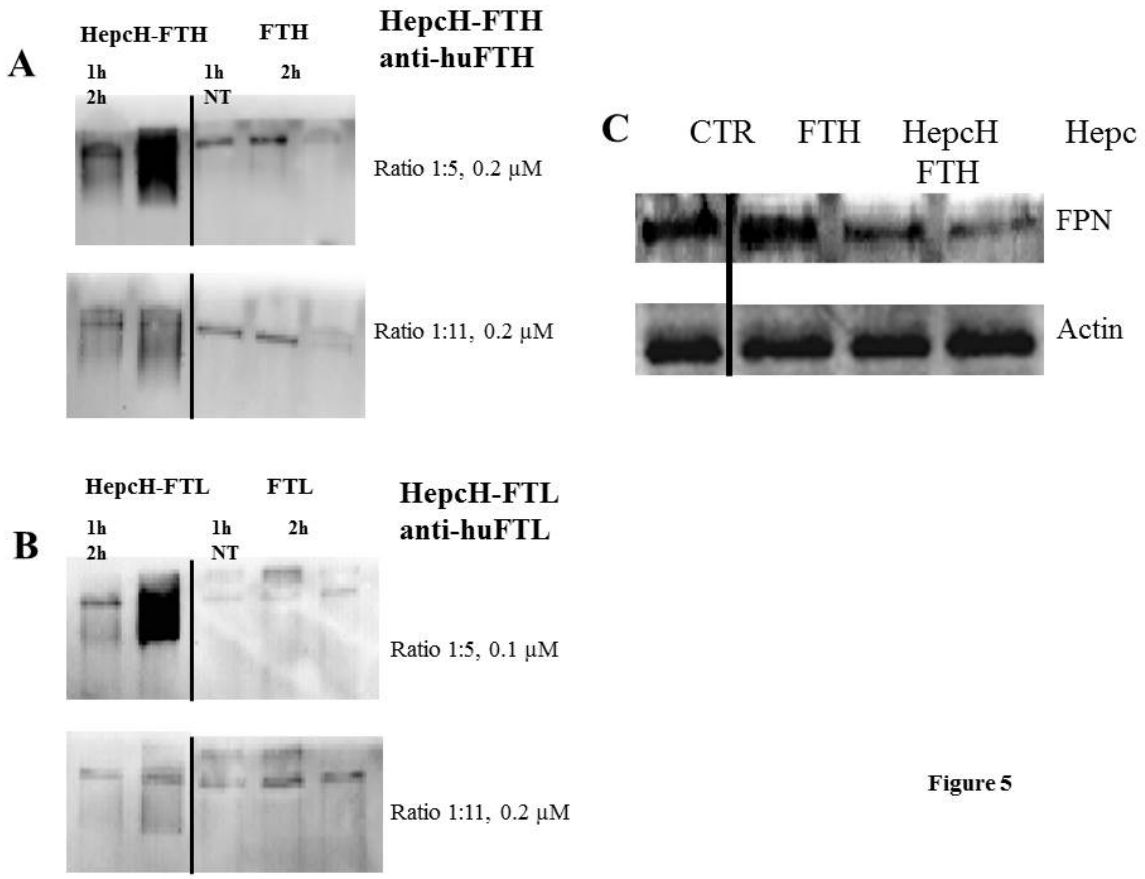


**Figure 5. HepcH-FTH heteropolymers bind iron treated J774 cells and cause ferroportin degradation**. A: Western blotting analysis of the non-denaturing PAGE of cell lysates after treatment with 0.2 µM HepcH-FTH (1:5 and 1:11) during 1 h and 2 h incubation using monoclonal anti-human FTH antibody. B: Western blotting analysis of the non-denaturing PAGE of cell lysates after treatment with 0.1 µM and 0.2 µM HepcH-FTL (1:5 and 1:11) during 1 h and 2 h incubation using monoclonal anti-human FTL antibody. Controls containing 0.2µM of native huFTH, and 0.1 µM and 0.2 µM of native huFTL were incubated at same final volumes and same reaction times with cells. NT, non-treated cells used as control. C: Western blotting analysis of the SDS-PAGE of cell lysates using polyclonal anti-rabbit ferroportin antibody. CTR: untreated cells. FTH: cells treatment with 0.5 µM native FTH for 2 h. HepcH-FTH: cells treatment with 0.2 µM HepcH-FTH (1:5) for 2 h. Hepc: cells treatment with 0.5 µM synthetic human hepcidin-25 for 2 h. Non-adjacent bands, from the same blot, were denoted by vertical black lines.

**Supplementary data**

**Table S1. Primers used in this study.**

| Primers | Sequence 5' to 3' | Using |
|---|---|---|
| NheI hFTH F | *CAAATG***GCTAGC**ACGACCGCGTCCA | huFTH construct |
| BamHI hFTH R | *TCGAG***GGATCC**CCGGGTTAGCTTTCATT | huFTH construct |
| NheI H25 F | *ATAGAC***GCTAGC**ATGGACACCCACTTCCCCATCTGC | HepcH construct |
| NheI H25 R | *ATAGAC***GCTAGC**GGTCTTGCAGCACATCCCAC | HepcH construct |
| pASK F | GAGTTATTTTACCACTCCCT | Sequencing |
| pASK R | CGCAGTAGCGGTAAACG | Sequencing |

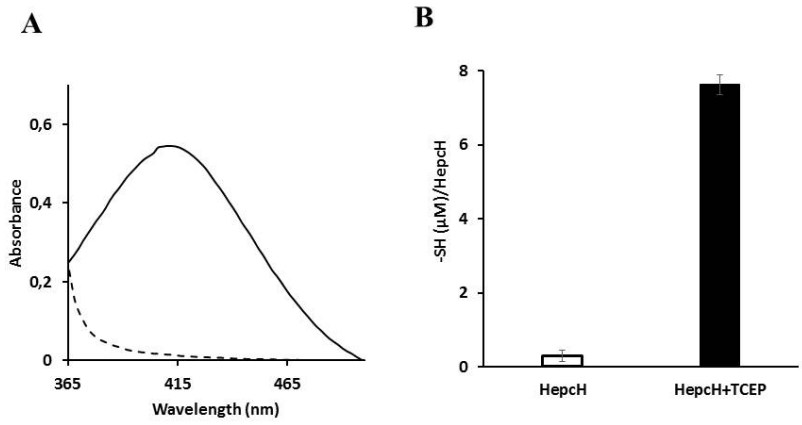


**Figure S1. Thiol quantification on the solubilized HepcH monomer. iron**

A: UV-vis spectra showing the results of Ellman's assay for thiol detection in the solubilized HepcH monomer (dashed) and the HepcH monomer subjected to reductive treatment (black line). Spectra show the appearance of an absorption band at 412 nm after reductive treatment in HepcH revealing the presence of cysteine sulfhydryl-groups. B: Amount of free sulfhydryl-groups per HepcH present in HepcH after reduction (black) and in the solubilized HepcH (white).

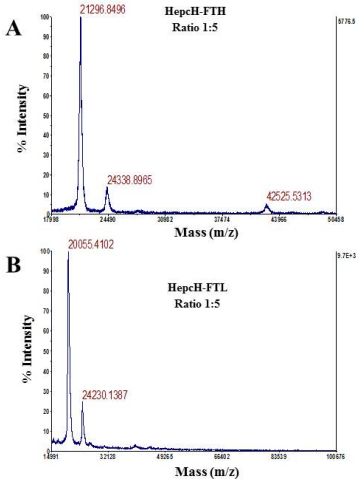


**Figure S2. MALDI-TOF spectra of the assembled HepcH-FTH (A) and -FTL (B) heteropolymers (ratio 1:5).**